

See discussions, stats, and author profiles for this publication at: <https://www.researchgate.net/publication/231371440>

Kinetic Studies of Low Severity Visbreaking

ARTICLE *in* INDUSTRIAL & ENGINEERING CHEMISTRY RESEARCH · FEBRUARY 2004

Impact Factor: 2.59 · DOI: 10.1021/ie0305723

CITATIONS

28

READS

121

5 AUTHORS, INCLUDING:



Aniruddha Pandit

Institute of Chemical Technology, Mumbai

320 PUBLICATIONS 9,162 CITATIONS

SEE PROFILE

Kinetic Studies of Low Severity Visbreaking

Kamal L. Kataria,[†] Rohit P. Kulkarni,[†] Aniruddha B. Pandit,^{*,†}
Jyeshtharaj B. Joshi,[†] and Manmohan Kumar[‡]

*Institute of Chemical Technology, University of Mumbai, Matunga, Mumbai - 400 019, India, and
Indian Institute of Petroleum, Dehradun, India*

Thermal cracking of vacuum residues and asphalts obtained from operating Indian refineries were studied in a batch reactor. The temperature was varied in the range 400–430 °C, and the batch time was varied from 0 to 15 min. The pressure was kept at a constant value of 1.2 MPa through out the experiment. The variation in the composition of the cracked gas fraction for each feed was studied by gas chromatography. The resulting visbroken products were further characterized in terms of its different industrially important boiling cuts. A five lump kinetic model, comprising of gas (C₁–C₅), gasoline (IBP–150), LGO (150–350), VGO (350–500), and VR (500+) has been developed. The variation in the kinetic parameters with change in the feed properties has been discussed. Also, an attempt has been made to seek a relationship between the feed properties with the kinetic rate parameters and the activation energies.

1. Introduction

Thermal cracking of heavy oils and vacuum residues has been advanced as an up-gradation process so as to meet the increasing demand for lighter fuels. Thermal cracking by carbon rejection methods such as visbreaking, delayed coking, and resid catalytic cracking and hydrogen addition methods such as hydrovisbreaking, hydrocracking, etc. are some of the important residue up-gradation processes. In these methods, visbreaking and delayed coking contribute about 32 and 30% respectively in terms of the total residue volume processed. These are followed by hydroprocessing and residue FCC with respective contributions of 19 and 15%. Deasphalting, the physical method of residue processing, contributes the remaining 3.5%.¹ Visbreaking, a viscosity reduction process, is a mild liquid phase pyrolysis of large molecules to smaller ones to form lighters and gaseous products and offers some additional benefits. The process severity is controlled by the interchangeable operational variables (being essentially a first-order reaction) such as temperature and the residence time. In the past decade, most of the visbreaking units have been modified from coil-type (high temperature and lower residence time route) to coil-soaker (high residence time and lower temperature route), thereby reducing the process temperature by about 10 °C. This modification has enhanced the yields of gas and gasoline. Further, the concurrent visbroken products obtained attain a relatively superior quality of the fuel oil and require zero to low quantity of cutterstock for property adjustments.

For a given feed, the extent of conversion, selectivity to gas and gasoline, coking behavior, and stability of the visbroken product are directly related to the feed characteristics, such as paraffin, asphaltene content, aromaticity, heteroatom content, etc., and vary to a large extent from feed to feed. The extent of conversion of a particular feed within the stability range is called the crackability of the feed.² To investigate the role of feed properties on the crackability, several re-

search groups^{3–13} have studied the kinetics of visbreaking of heavy oils and residues from a large number of sources in a batch or continuous manner. These studies were primarily focused on thermal cracking behavior of feeds such as (i) model compounds having characteristics similar to heavy oil (average boiling point, viscosity, etc.) and (ii) actual heavy oils that includes atmospheric residue (AR), vacuum residue (VR), and their blends which act as major feeds for the visbreaking units.

The residue is composed of complex organic components, and it is difficult to develop a mechanistic approach for each molecule to explain the true kinetics and their thermal behavior. Thus, the pseudo-components are obtained by group composition based on their physicochemical properties such as boiling points, solubility, etc. The reported lumped kinetic models can be categorized into (i) parallel reaction models (Table 1) and (ii) parallel-consecutive reaction models (Table 2). A summary of the above-mentioned research can be listed as follows.

1. During thermal cracking, paraffins mainly undergo C–C splitting while asphaltenes follow dealkylation reactions.^{6,10}

2. The crackability of the feed was found to be a linear function of difference in the aromatic content of the asphaltenes and maltene phase.⁶

3. Gas composition was found to be independent of severity.^{10,11}

4. The observed nonlinear trends for the distillate products were mainly due to onset of condensation reactions beyond certain severity.⁴

5. The activation energy was found to vary with the feed properties (such as percentage of saturates, polar aromatics and asphaltenes present, CCR, sulfur, and metal content). Activation energies for the cracking and condensation reactions were estimated to be in the ranges 14–78 and 17–60 kcal/mol, respectively. Such a large variation in the activation energy can be attributed to the large structural variation within the lump considered and the degree of lumping.

The above studies are reported for higher severity range where cracking and condensation reactions may compete with each other. The theoretical residence time and severity covered in the commercial coil-soaker

* To whom correspondence should be addressed. Tel.: 91-22-2414 5616. Fax: 91-22-2414 5614. E-mail: abp@udct.org.

[†] University of Mumbai.

[‡] Indian Institute of Petroleum.

Table 1. Summary of Previous Work on Proposed Parallel Kinetic Models

Summary of previous work on proposed parallel kinetic models					
Authors	Feed	Experimental Details		Model	Conclusions
Al-Soufi et al. ³	Heavy Iraqi residue (350°C+, Asphaltene 9.5%)	Reactor	Pilot plant Coil-Soaker type		1. Within the severity range covered, thermal cracking follow first order 2. E- 23.7 kcal/mol
		Temp. (°C)	435-480		
		Res. time (min)	Coil 0.72–1.81 Soaker 2.5–6.3		
		Pressure (MPa)	0.7		
Krishna et al. ⁴	Aghajari long residue (370°C+, CCR-7.9)	Reactor	Bench scale unit		1. Within the severity range covered, thermal follow first order 2. E- 53.4 kcal/mol A- $2.17 \times 10^{12} \text{ s}^{-1}$
		Dimensions	Coil 6 mm i.d. Length 1.6 m		
		Temp. (°C)	427-500		
		Flow rate (l/h)	2.04-2.91		
		Pressure (MPa)	1.7		3. Secondary cracking of the products starts beyond 7% conversion.
Castellanos et al. ⁵	Maya & Isthmus AR, VR	Reactor	Industrial Dubb's Unit		1. Under industrial operating conditions feed follows first order thermal cracking. 2. The model predicts the yields of industrial units and have been used successfully for design purpose.
Di Carlo and Janis ⁶	Rospo dimare, Balayam, Es sider atm. Residue (nC ₇ -insoluble s-32.3, 5.8, 1.8 wt.% resp.)	Reactor	Pilot plant (coil type)		1. Thermal cracking were found to be first order. 2. Activation energies (E) were found to be 31.3, 68.0 and 78.8 kcal/mol for Rospo di mare, Belaym, Es Sider respectively. 3. Paraffins undergo C-C splitting while aromatic molecules undergo dealkylation 4. The crackability of the feed was proportional to the difference between the aromaticity of the asphaltene and maltene phase.
Benito et al. ⁷	Asphaltic coal residue (Spanish coal)	Reactor	Steel tubular reactor 13 mm id Length 0.4m		1. First order thermal cracking 2. For the studied feed, rate of condensation to yield coke was found to be higher than the cracking rate to yield lighters 3. The estimated activation energy for cracking and condensation were found to be 14.6 kcal/mol and 17.2 kcal/mol respectively.
Xiao et al. ⁸	Heavy oil	Reactor	Micro-reactor (20 g)		1. The overall conversion was based on the obtained 500- distillates 2. The proposed model was based on the pseudo components based on their boiling cuts 3. It was assumed that the formed distillates do not undergo further cracking and thus linear regression was applied to estimate the rate parameters. 4. The overall activation energy for the conversion of residue to 500- distillates was 65.79 kcal/mol

visbreaker units are relatively low (typical range of residence time is; coil 2–4 min and soaker 20–25 min), and hence the estimation of initial cracking rates is essential. In the present work, the variations in the yields of the products and kinetic parameters with the change in the feed properties for different types of feeds processed in the operational visbreaker units of Indian refineries were aimed to study. Six different feeds including vacuum residues and PD asphalts obtained from the operational Indian refineries covering wide range of physicochemical properties were studied.

3. Characterization of Feedstock

The vacuum residues, North Gujarat Short Residue (NGSR), Bombay High Short Residue (BHSR), Arab Mix

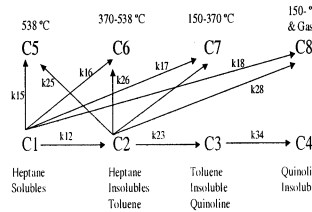
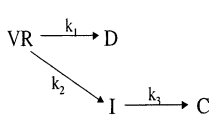
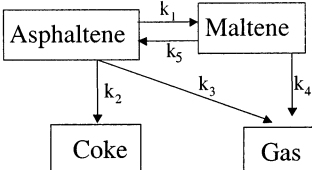
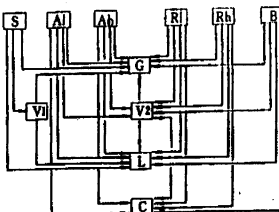
Short Residue (AMSR), VB Feed Mathura, and two PD asphalts, Haldia Asphalt and AM Asphalt, were procured. The residues were characterized as per the standard ASTM and IP methods. [The data VB Feed has been taken from Singh,¹⁴ as it is also available in the same format as required for the present analysis.] Table 3 summarizes the properties of each of the residue studied. Thermal cracking behavior of a particular feed being a strong function of its characteristic properties; the results obtained can be generalized for any feed within the range covered.

4. Experimental Section

4.1. Setup. All the experiments were performed in a batch mode. Figure 1 gives the schematic diagram of

Table 2. Summary of the Reported Parallel Consecutive Kinetic Models

Summary of the reported parallel consecutive kinetic models

Authors	Feed	Experimental Details	Model	Conclusions
Takatsu- ka et al. ⁹	Residual oil	Reactor: Flow reactor, Semi-batch, autoclave Temp. (°C): 400-450 Res. time (min): 0-450 Pressure (MPa): 0.013-0.45		<ol style="list-style-type: none"> 1. Atmospheric equivalent temperature and hydrocarbon partial (HC) pressure were incorporated to estimate Arrhenius rate parameters. The reaction model was found to represent the degree of cracking over wide range of operating conditions 2. Higher HC partial pressure decreases the reaction rate of polycondensation reactions; while degree of cracking increases with increasing reactor pressure 3. Polycondensation reactions proceed via consecutive reaction mechanism are greatly affected by RTD to yield higher content of quinoline insoluble pitch in product. 4. The estimated values of activation energies for cracking reactions were 60 kcal/mol while 40-50 kcal/mol for polycondensation reactions.
Del Bianco et al. ¹⁰	Belaym vacuum residue (CCR- 20.8 wt. %)	Reactor: Batch Reactor Temp. (°C): 410-470 Res. time (min): 0-120 Pressure (MPa): 1 (N ₂ atm)		<ol style="list-style-type: none"> 1. Coke is formed only via intermediate 2. E₁-49.4 kcal/mol; A₁-31.97 min⁻¹; E₂-63.9 kcal/mol; E₃-40.92 min⁻¹ 3. Gas composition remained unchanged for the covered severity 4. Structural study shows that thermal cracking of asphaltenes follows dealkylation reactions 5. Condensation reaction prevail at high severity levels
Trauth et al. ¹¹ and Yasar et al. ¹²	Honda, Maya, Arabian light, Arabian Heavy residue & their isolated asphalt- enes	Reactor: Thin walled glass test tube Temp. (°C): 400-450 Res. time (min): 20-180 Pressure (MPa): 0.5 (N ₂ atm)		<ol style="list-style-type: none"> 1. The reactivity was found to be proportional to the asphaltene content and their aromaticity and thus HR > AHVR > MR > ALR 2. The kinetic parameters for the four limped five rate parameters were estimated for residues and isolated asphaltenes 3. The activation energy of HR and ALR, were found be higher than their respective isolated asphaltenes for all reaction pathways.
Zhou et al. ¹³	Daqing, Guanshu and Liaohe short residue	Temp. (°C): 400-460 Res. time (min): 0-90		<ol style="list-style-type: none"> 1. Three different residues were separated into six pseudo components of saturate, light and heavy aromatics, light and heavy asphaltenes based on their solubility in different solvents. 2. The separated fractions were studied for their thermal behavior separately and resulted to their inter-conversion

the experimental setup. The reactor used was a horizontal 400 mL SS-316 bomb, with the provision of measuring the liquid and vapor temperature. The reactor was pressurized with nitrogen and was maintained with the help of a pressure-regulating needle valve. The molten salt (eutectic mixture of KNO₃, NaNO₃, and NaNO₂ with 53, 7, and 40 wt %, respectively) bath was used as the heating medium. The cold trap was used to separate the gas from the entrained lighters. A gas meter was used to quantify the extent of gaseous products.

4.2. Experimental Procedure. The molten salt bath was heated electrically and the temperature was controlled within ± 2 °C using a PID controller. The bath temperature was kept always higher by 50 °C than the desired reaction temperature so as to maintain the thermal gradient. The reactor was charged with approximately 120 ± 0.5 g of the sample and was pressurized with N₂ at room temperature to 0.6 MPa g. Since the cracking reactions start at around 350 °C and the

desired reaction temperature was in the range of 400–430 °C for the residence time of 0–15 min, it was necessary to shorten the heating time. For this purpose, the heating was carried out in two stages. In the first stage, the reactor was placed just above the molten salt surface so as to preheat the residue to 300 °C using the convective heat of the salt bath. As soon as the liquid attained 300 °C, the reactor was dipped in the molten salt bath with constant rocking of the reactor so as to assure uniform mixing of the residue. The reaction temperature was attained in a time period of 1.5–2 min. The temperatures of the liquid and vapor fraction were measured simultaneously at an interval of 15 s. The reactor attained an absolute pressure of 1.2 MPa before the reaction temperatures were reached. The excess pressure in each run was released and was maintained at a constant value of 1.2 MPa using the pressure-regulating needle valve. The gas and the entrained lighters (low boiling fractions) were passed through the

Table 3. Properties of Feedstock

property ^a	NGSR	BHSR	AMSR ⁴	VB Feed ¹	Asphalt	AM Asphalt
source	IOCL, Gujarat	BPCL, Mumbai	HPCL, Mumbai	IOCL, Mathura	Haldia Refinery	HPCL, Mumbai
1 density, d_4^{15}	0.9747	0.9636	1.0232	1.0176	1.054	1.0430
2 kinetic viscosity, cSt						
at 100 °C	1501.27	91.3	1084.10	526.5	8217.3	2444.90
at 135 °C	272.55	24.4	168.49	102.3	690.7	286.4
3 S, wt %	0.27	0.45	4.43	4.29	4.93	5.11
4 N, wt %	0.538					
5 CCR, wt %	14.77	12.8	21.10	19.8	25.7	30.6
6 C/H ratio		5.58	6.59	7.50	7.78	
7 mol wt		793.5	800.2	871.5	1078.8	1193.0
8 nC_5 insol. wt %	11.24	7.25	16.19	13.19	26.92	17.25
9 nC_7 insol. wt %	6.01	4.46		8.90	12.70	9.812
10 asphaltenes, wt %	1.85	3.03	6.50	7.72	10.15	9.606
11 pour point, °C	+48	+69	+42	+39	+72	+60
12 metals, ppm						
V	2.60	3.40	9.00	29.30	95.75	94.70
Ni	207.0	24.95	21.65	36.55	46.30	26.40
Fe	119.0	8.30	82.00	22.90	30.80	13.90
13 H-C type analysis, wt %						
saturates	10.30	32.89	15.00	14.76	5.63	5.12
naph. arom.	58.31	59.82	66.60	67.85	68.07	66.05
polar arom.	29.10	4.23	6.74	6.40	11.86	17.81
nC_7 insol.	2.11	3.03	11.00	10.47	13.69	10.9

^a All the tests were performed as per the ASTM/IP methods.

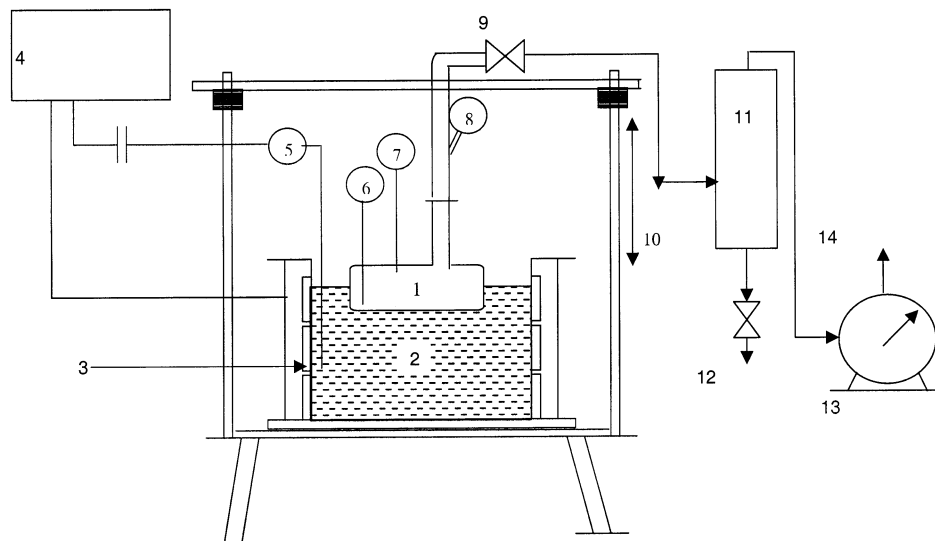


Figure 1. Schematic diagram for experimental setup for the batch studies: (1) SS-316 reactor (400 mL capacity); (2) molten salt bath (eutectic mix); (3) electric heaters; (4) furnace control for salt bath; (5) bath thermocouple and temperature indicator; (6) liquid thermocouple and temperature indicator; (7) vapor thermocouple and temperature indicator; (8) pressure indicator; (9) pressure release needle valve; (10) vertical movable stand for reactor; (11) cold trap for lighters; (12) lighters collector; (13) gas meter; (14) gas outlet

cold trap maintained at the temperature of about 1–3 °C. The total volume of the gas after the cold trap was measured using a gas meter and was then collected in a gas sampling tube for further analysis. The reaction temperature of the liquid through out the run was maintained constant by adjusting its position in the salt bath (extent of dipping). After the desired reaction time, the reactor was immediately removed from the salt bath and dipped in the water bath at 25 °C to quench the reaction. This quenching period was approximately 3–4 s. The reactor was then slowly depressurized to atmospheric pressure and the entrained vapors and gaseous products were passed through the cold trap followed by the gas meter. The condensates and gaseous products were collected and quantified separately. The volume of the nitrogen was subtracted from the measured cumulative volume of the gaseous products so as to obtain the volume of the formed gaseous products during the reaction. The left visbroken tar in the

preweighed reactor was collected and weighed in a distillation flask for further analysis. The reactor was again weighed so as to account for the uncollected material. The material balance was accounted in terms of quantities of gaseous products, condensates and visbroken tar and was always within 99%. The final data reported here for each run is the average of three to four runs under identical conditions and the observed deviations in the yields were always within $\pm 5\%$.

4.3. Reaction Scheme. The reaction scheme was based on the conversion of the residue in terms of the fraction boiling below 500 °C. The feed was first characterized in terms of its physicochemical properties. The characterized feed was then subjected to thermal cracking using above apparatus and procedure. The gas fractions were analyzed by chromatography. Thermally cracked reaction mixture was separated by distillation to atmospheric distillates (fraction boiling up to 150 °C), mid-distillates (fraction boiling up to 300 °C at 15

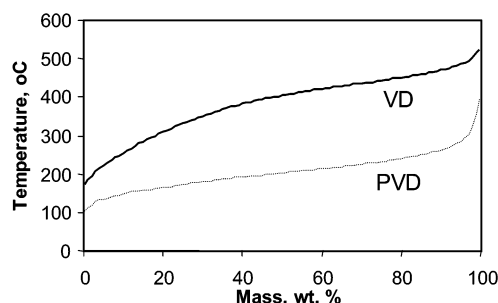


Figure 2. Typical TBP curve obtained for the prediction of the different boiling cuts.

mmHg pressure) and finally the vacuum gas oil (fraction boiling up to 500 °C at a pressure of 0.2 mmHg). The separated distillates were subjected to SIMDIST analysis to obtain their SIM-DIST boiling point curve. The left out 500+ visbroken residue was then analyzed for its stability.

4.4 Analysis of the Reaction Products.

Gas Analysis. The gas fraction was analyzed using simple gas chromatography (GC), also called a refinery gas analyzer (RGA), equipped with a packed column (30% squalene, 5 m) and flame ionization detector (FID).

Distillates Analysis. Two samples comprising (i) the mixture of atmospheric distillates and the mid-distillates and (ii) vacuum distillates were analyzed separately using simulated distillation (SIMDIST). The SIMDIST was operated as per the ASTM Ext. D-2887 method using HP-6890 series GC equipped with fused silica column (cross-linked methyl silicone gum) of 10 m \times 0.9 μ m \times 0.53 μ m and CS₂ as diluent. The TBP curves were obtained by the above analysis for each run (Figure 2) and were used to predict the weight fractions of different pseudo-boiling-components considered in the reaction scheme.

Stability Test. The feed residue and the visbroken residue (500+) obtained by the above distillation were analyzed for their stability by the standard merit number test (IFP-3024-82, severity test for thermal reactions by spot method and residue stability determination). For this purpose, a 2 mL sample was diluted with 10 mL of a mixture of *o*-xylene and 2,2,4-trimethylpentane with variable *o*-xylene content. The above mixture of the sample and the diluent was homogenized with the help of a glass rod. The homogeneous mixture was spotted on Whatman filter paper no. 2. The spot was visually evaluated for its homogeneity or phase separation. For homogeneous samples, the stability is indicated by the lowest volume of *o*-xylene added in a mixture of *o*-xylene and 2,2,4-trimethylpentane. The spot with a markedly darker center (appearance of two phases) was considered to be an unstable sample. Samples with merit numbers less than 7 are considered to be stable samples while those with merit numbers in the range 7–8 are taken as borderline, and above 8, the samples are said to be unstable. For necessary fuel oil specifications, the merit number test is carried out for 150+ or 350+ bottoms fraction. However in the present case for the 500+ visbroken residue, samples having a merit number less than 6.5 were considered as stable samples while those with a number above 6.5 were considered to be unstable. The typical images of stable and unstable samples of visbroken residue (500+) are shown in Figure 3.

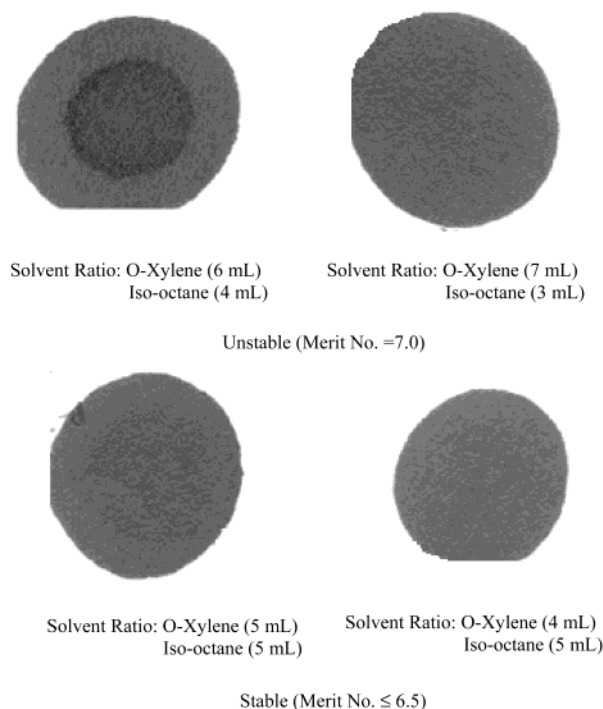


Figure 3. Merit number test for stability of the VR (500+): (A) experimental feed, 500+ sample of AM Asphalt, $T = 420$ °C, RT = 15 min; (B) experimental feed, 500+ sample of AM Asphalt, $T = 420$ °C, RT = 9 min.

5. Results and Discussions

The main aim of the present work was to determine the variation in the cracking behavior as a function of the feed characteristics, effect of higher asphaltene content, to evaluate the rate parameters for each feed and to find the dependency of the reaction rate parameters on the feed characteristics.

Conversions of Vacuum Residues and Asphalt. Thermal treatment of the feed leads to the formation of components boiling below the initial boiling points (IBP) and this variation was considered as the basis for the conversion. Thus, the conversion was based on the products having a boiling range below 500 °C.

$$\text{total conversion (\%)} = \left(\frac{W_{\text{gas}} + W_{500-}}{W_{\text{feed}}} \right) 100 \quad (1)$$

$$\text{yield (\%)} = \left(\frac{W_i}{W_{\text{gas}} + W_{500-}} \right) 100 \quad (2)$$

The thermal cracking of VR resulted in its conversion to distillates (below 500 °C) showing a linear decline in the concentration with a rise in the reaction temperature and/or the time (Figure 4). At lower temperatures (400 and 410 °C), the linear gradient in concentration was observed as compared to steep gradients in the case of higher temperatures (420 and 430 °C). The further comparison of the relative rates of cracking for different feeds on the basis of their rate constants is discussed in a later section.

Gas Component. The analyses of the gaseous products for each feed are given in Table 4. The analysis was done only for the HC gaseous components. However, the gases H₂S, CO, and CO₂ that are also found to be present in the visbreaker gas were not analyzed, and thus the results shown should be considered as

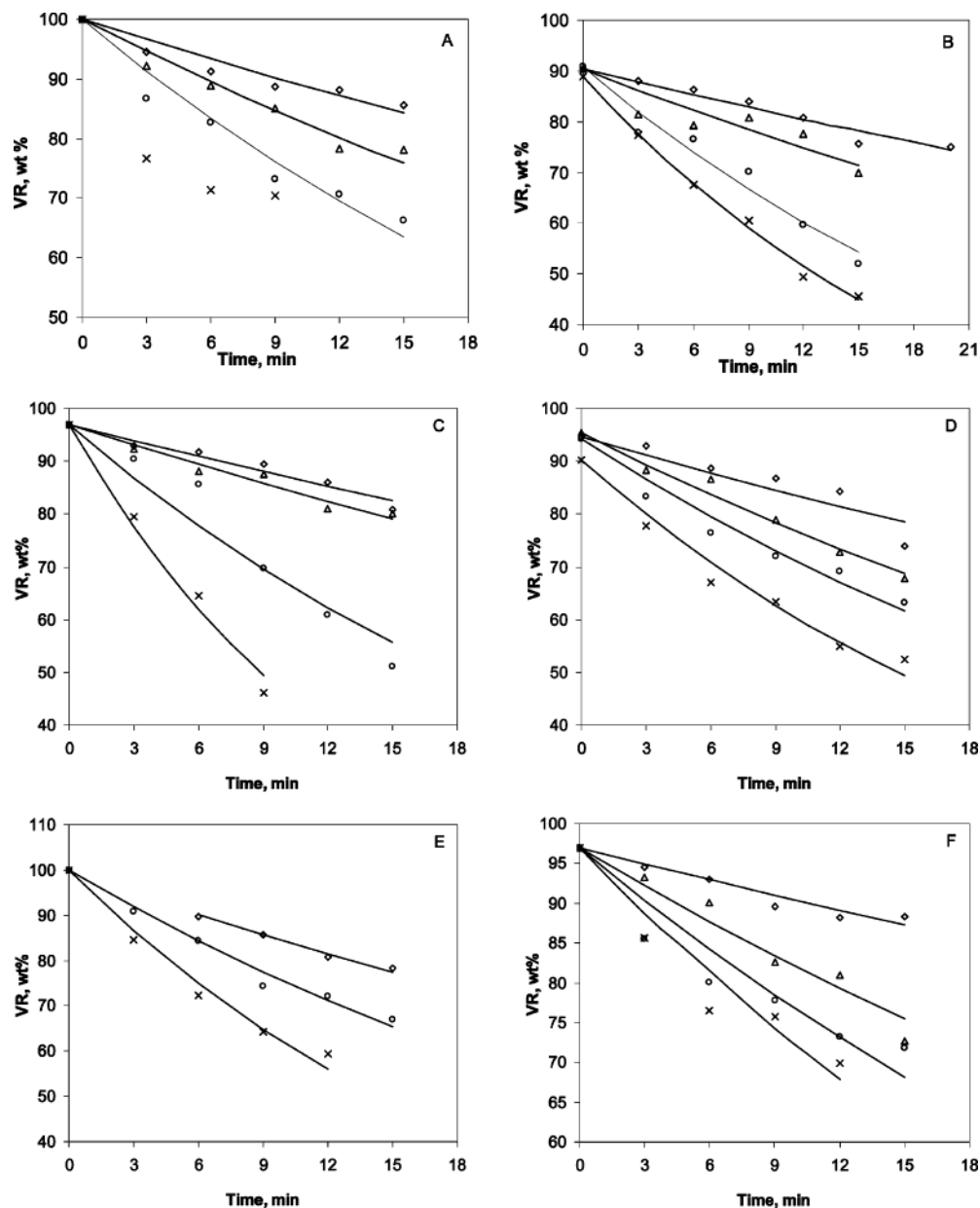


Figure 4. Experimental and predicted conversion of VR (500+) at various temperatures; (A) NGSR; (B) BHSR; (C) AMSR; (D) VB Feed; (E) Haldia Asphalt; (F) AM Asphalt; \diamond , 400 °C; \triangle , 410 °C; \circ , 420 °C; \times , 430 °C

Table 4. Gas Components Obtained by Refinery Gas Analyzer

gas component	NGSR	BHSR	AMSR	VB Feed		AM Asphalt
				400 °C, 15 min	430 °C, 15 min	
C_1	31.4	46.00	29.64	38.21	32.82	48.14
$iC_2=$	3.65	2.26	2.00	1.94	2.09	2.71
C_2	16.76	15.13	18.45	19.36	19.41	18.98
$C_3= + C_3$	30.79	24.55	26.47	19.06	19.97	19.66
iC_4	2.13	2.14	1.58	1.95	2.23	1.02
nC_4	4.87	4.76	7.59	8.09	9.07	2.37
$C_4=$	3.04	2.50	5.69	4.82	6.00	4.40
iC_5	2.13	1.07	3.37	6.55	8.38	1.02
nC_5	2.74	1.07	3.37			1.02
$C_5=$	2.43	0.476	1.79			0.68
tot.	100	100	100	100	100	100
av mol wt	28.56	33.4	35.52		36.18	28.98
ρ_{av} (kg/m ³)	1.275	1.49	1.58		1.61	1.294

^a $C_2=$ = olefinic.

semiquantitative. The following results can be concluded from the analysis of the gas (G) fraction for all the feeds.

1. The yield of gas fraction increases as the severity increases. This is in agreement with the previous work on Belaym VR¹⁰ and Arabian Light Asphalt.¹²

2. In visbreaker gas, methane was obtained as a major fraction. The gas analyses obtained by visbreaking of Maya, Hondo, Arabian Light Asphalt,¹² and VR processed by Maxa et al.¹⁵ have shown similar results.

3. For vacuum residues, the average molecular weight of the gas fraction increases with increasing asphaltene content.

4. At high severity, there is a slight increase in the C_3 , C_4 , and C_5 fractions. This indicates that, at low severity, first the lower alkyl chain component cracks, possibly from the asphaltenes (nC_5 insolubles); however, with an increase in the severity, the higher component fractions begins to crack. Their proportions may slightly vary for a given feed for a commercial visbreaker unit usually operated at higher severity.

Distillate Component. The distillates obtained were fractionated into three boiling cuts; gasoline (Ga, IBP-

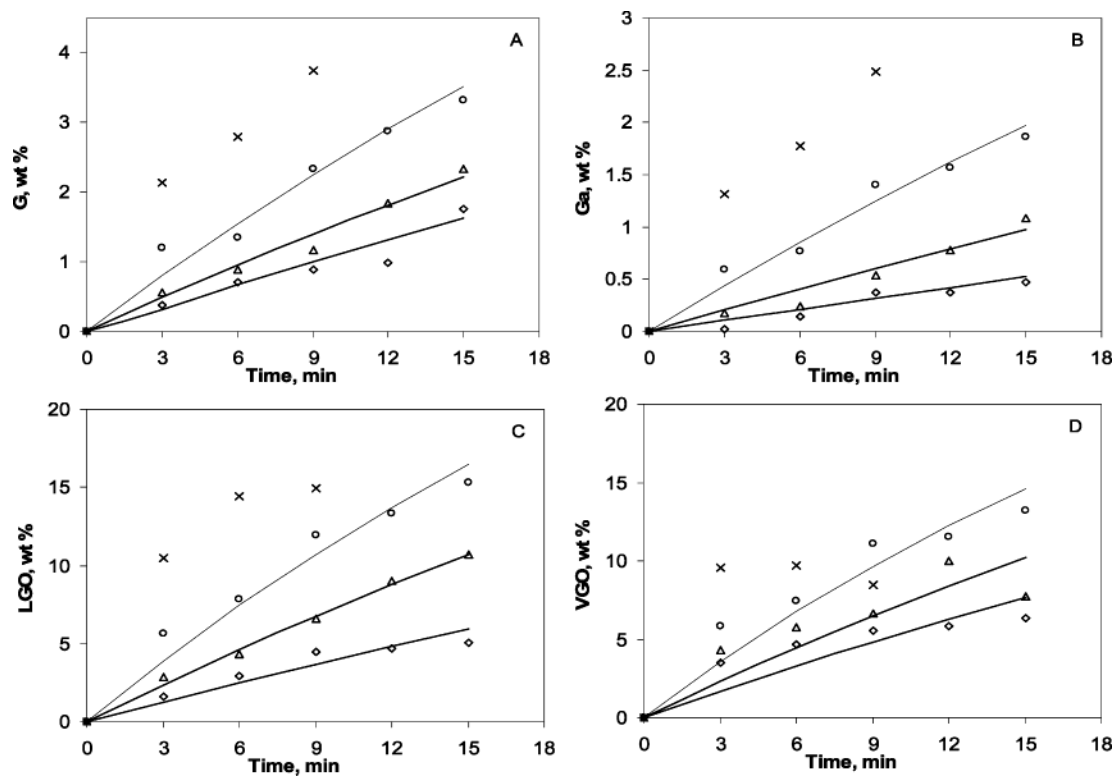


Figure 5. Comparison between experimental and predicted values of various components for NGSR: (A) G; (B) Ga; (C) LGO; (D) VGO; \diamond , 400 °C; \triangle , 410 °C; \circ , 420 °C; \times , 430 °C.

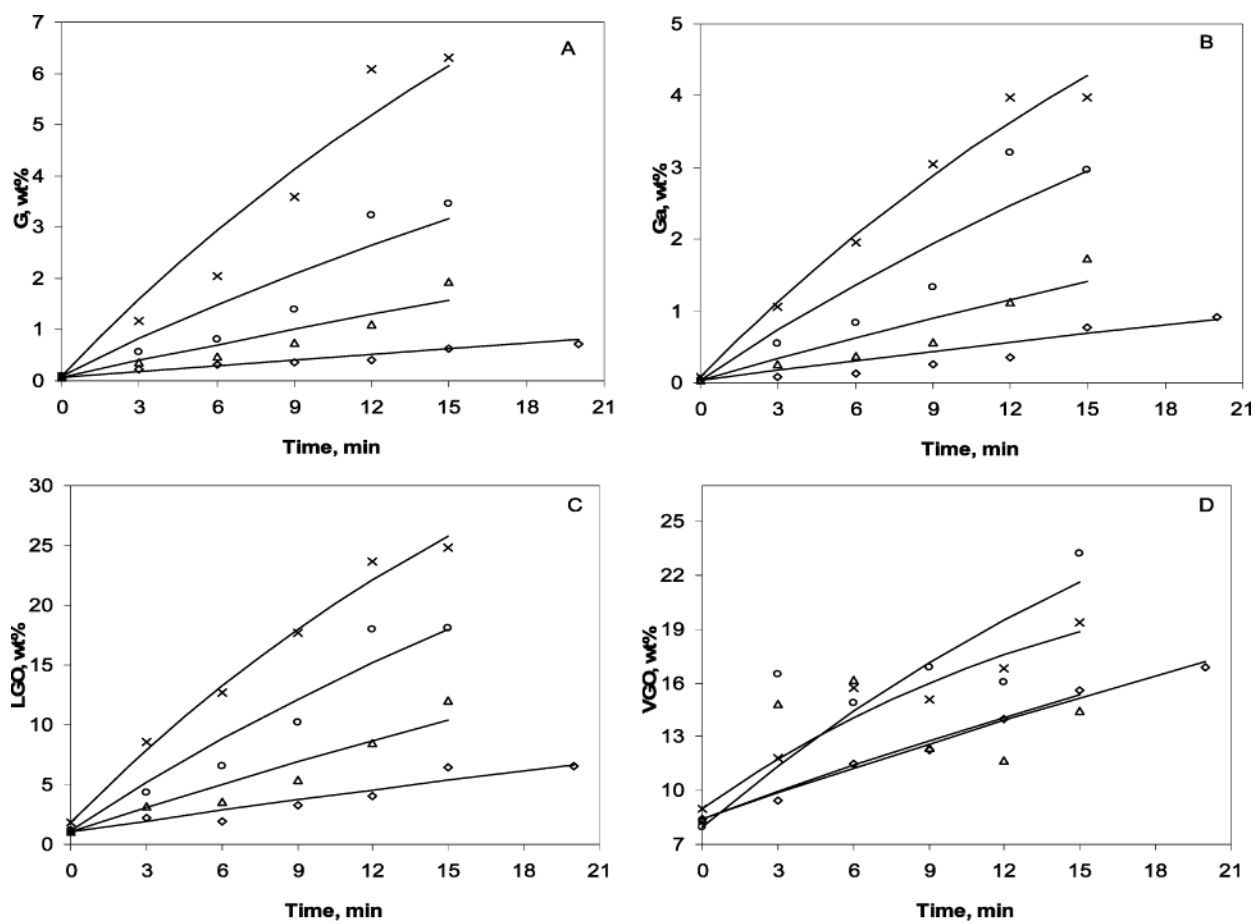


Figure 6. Comparison between experimental and predicted values of various components for BHSR: (A) G; (B) Ga; (C) LGO; (D) VGO; \diamond , 400 °C; \triangle , 410 °C; \circ , 420 °C; \times , 430 °C.

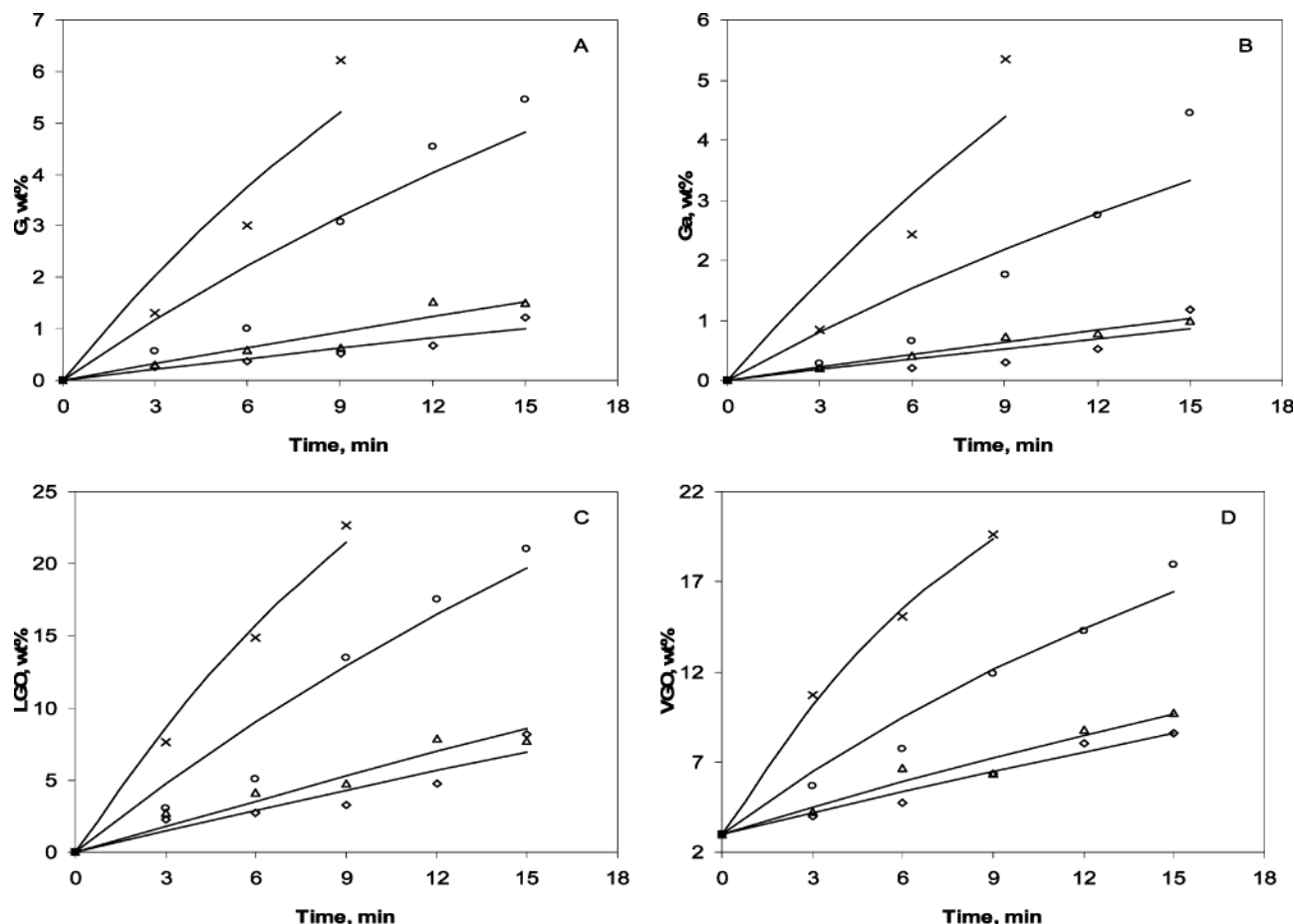


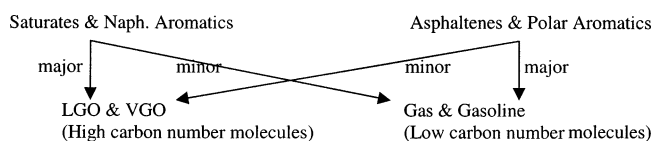
Figure 7. Comparison between experimental and predicted values of various components for AMSR: (A) G; (B) Ga; (C) LGO; (D) VGO; \diamond , 400 °C; \triangle , 410 °C; \circ , 420 °C; \times , 430 °C.

150 °C), light gas oil (LGO, 150–350 °C), and vacuum gas oil (VGO, 350–500 °C) by simulated distillation. The variations in the fractional yields obtained for each feed at different reaction temperature and residence time are shown in Figures 5–10. Initially, the yield of the VGO fraction was high followed by LGO, G, and Ga fractions for all the feeds. As the reaction proceeds (longer residence time), the yield of the VGO decreased continuously showing its cracking behavior under the range of the operating conditions. Similarly, in the case of LGO, the yield variation is linear at low severity levels for all the feeds; however, the extreme severity resulted to slight decline in their yields, which may be due to its subsequent thermal cracking. The observed linear trend for Ga and G for all the severity levels shows that these species are thermally stable and do not undergo further cracking. Two qualitative observations can be made from the above figures: (i) the threshold temperature above which the feed cracking initiates, highly depends on the feed type, e.g., Haldia asphalt showed no cracking at 400 °C at all residence time studied, and (ii) the different magnitude of relative rates of cracking/formation at a given temperature may be attributed to large compositional changes within a pseudo-cut.

For an industrial visbreaker unit, the ratio of G to Ga formation is, generally, 1:1 to 1:1.5. However, in the present case, this ratio was less than 1 for low severity and approached 1:1 at high severity range. At a low severity (typically for 3 min residence time at 400 and 410 °C), the small amount of formed gasoline lead to its improper removal from the tar during the distillation, which induced an error in its accountability. This

resulted in the deviation in G to Ga proportion in the present case.

On the basis of the study using structural analysis of the VR and visbreakates reported by Fainberg et al.¹⁶ and conclusions of Di Carlo and Janis,⁶ following mechanistic path for the components can be concluded:



Thus, the yields of the various products depend on their relative proportion and the extent of their crackability. In view of the above study, the five feeds covered in the present case and the data on VB feed (taken from the work of Singh¹⁴) can be divided into three major classes based on asphaltenes (As) to saturates (Sa) ratio⁶ as follows: (i) paraffinic feeds, e.g., BHSR, NGS, <0.5; (ii) intermediate asphaltenic feeds, e.g., VB Feed, AMSR (0.5–2.0); (iii) the asphaltenic feed, e.g., Haldia Asphalt and AM Asphalt (≥ 2).

The obtained product yields were correlated with (i) severity index, SI, defined on the basis of $E = 50$ kcal/mol and reference temperature of 700 K¹⁷ and (ii) feed properties such as wt % of Sa, NA, PA, As, nC_5 , CCR, S content, etc. Briefly the functional relationship can be stated as

$$\text{product yields (wt \%)} = f(\text{SI, feed properties}) \quad (3)$$

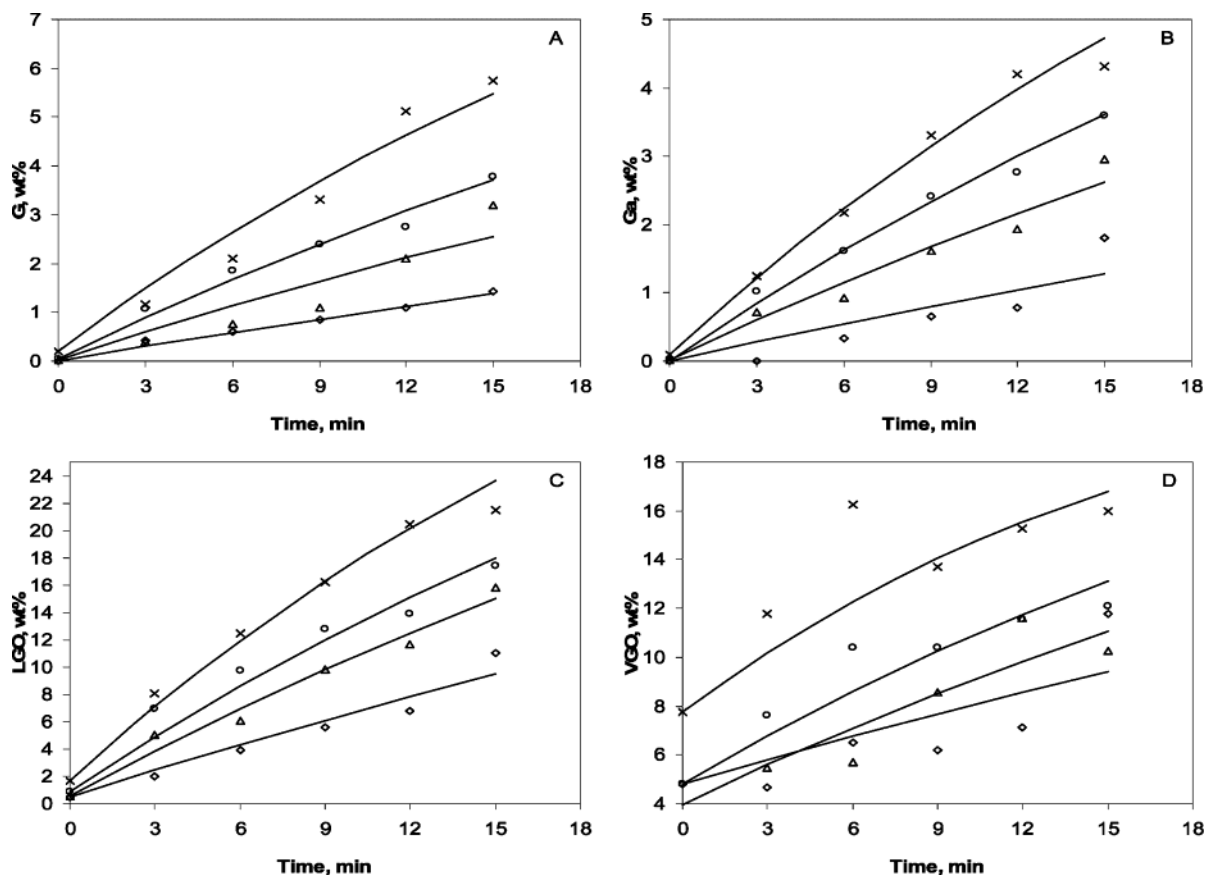


Figure 8. Comparison between experimental and predicted values of various components for VB Feed: (A) G; (B) Ga; (C) LGO; (D) VGO; \diamond , 400 °C; Δ , 410 °C; \circ , 420 °C; \times , 430 °C.

where

$$SI = t \exp\left(\frac{-E}{R}\left(\frac{1}{T} - \frac{1}{T_{700}}\right)\right) \quad (4)$$

The expression for normalized VR ($VR/VR_0 \times 100$) yield was found to be

$$VR = 100\left(\frac{As}{Sa}\right)^{0.02} \exp\left(-0.023\left(1 + \frac{nC_5}{CCR}\right)SI\right) \quad (5)$$

The exponential function of SI in the above equation represents the first-order cracking of VR very well. The terms (nC_5/CCR) and (As/Sa) denote the feed aromaticity, and the exponent, 0.02, for (As/Sa) depicts a weak function of this ratio.

The differential VGO yield was correlated as

$$VGO = 4.76(SI)^{0.5} \left(\frac{nC_5}{S + CCR}\right)^{0.96} R^2 = 0.71 \quad (6)$$

It shows a square root function of the severity while the feed property that influenced was found to be the ratio of $(nC_5/(S + CCR))$ with 0.96 as exponent. However, the poor correlation coefficient ($R^2 = 0.71$) obtained in the above expression may be attributed to the further cracking of VGO to low boiling products.

In the case of LGO, the following power-law relationship was found to hold:

$$LGO = 3.24(SI)^{0.77} \left(\frac{Sa}{NA}\right)^{0.13} R^2 = 0.88 \quad (7)$$

An exponent of 0.13 for the (Sa/NA) ratio indicates a

relatively weak dependency as compared to severity (exponent of 0.77). Thus, the formation of this species can be said to be more or less feed independent.

The formation of gasoline was found by the following power-law correlations:

$$Ga = 0.271(SI) \left(\frac{As}{PA}\right)^{0.19} R^2 = 0.83 \quad (8)$$

It shows that the gasoline formation is directly proportional to the SI and shows a moderate dependency over (As/PA) with an exponent of 0.19.

The yields of gas fraction were obtained in the following order: Haldia Asphalt > NGSR \approx AMSR > VB Feed > AM Asphalt \approx BHSR. On the basis of the above trend for the different feeds, the following correlation has been developed:

$$G = 0.43(SI) \left(\frac{nC_5}{CCR}\right)^{0.45} R^2 = 0.88 \quad (9)$$

The formation of gas was found to be proportional to the severity and also the nC_5 and CCR content of the feed. With an increase in nC_5 for a fixed CCR content of the feed, the yield of gas increases in approximately square root proportion.

The above correlations show that the newly defined group properties can satisfactorily represent the cracking behavior at least semiquantitatively within the studied range for which the parity plots for the same are shown in Figure 11. However, further improvements in the above correlations to correctly depict the feed dependency and deviations requires (i) the detail analysis of the lumps such as variation in their molecular

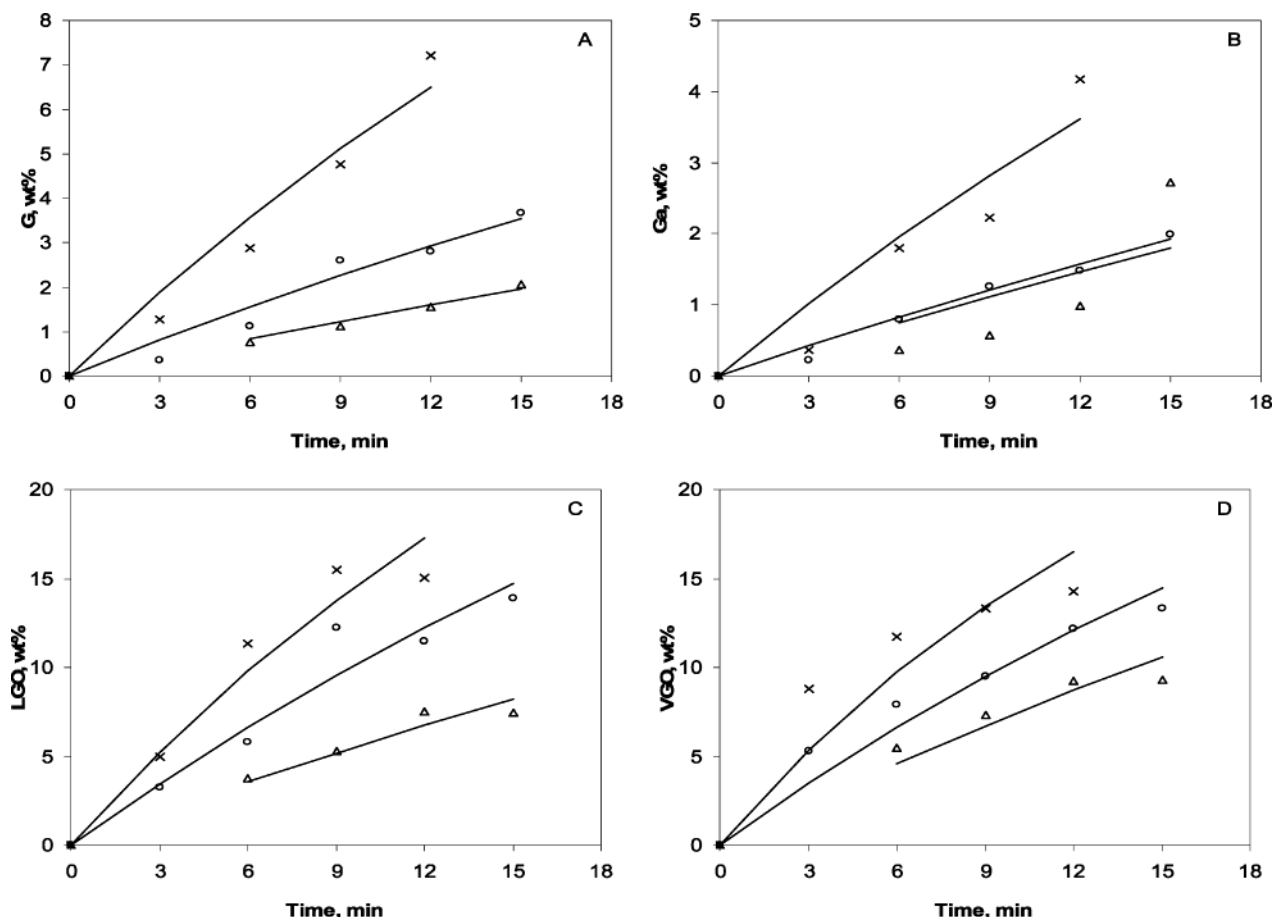


Figure 9. Comparison between experimental and predicted values of various components for Haldia Asphalt: (A) G; (B) Ga; (C) LGO; (D) VGO; Δ , 410 °C; \circ , 420 °C; \times , 430 °C.

weight, side chains, and aromatic index so that the empirical molecular components arising from each lump can be obtained and (ii) incorporation of the secondary cracking of VGO into lower boiling components.

The extent of the permissible conversion for a given feed by the visbreaking process is controlled by the stability of the visbroken tar and its coking propensity.¹⁷ These parameters are directly related to the feed characteristics and in particular to its asphaltene content and the relative stability of the asphaltene in the maltene phase. The stability of the feed not only depends on the asphaltene content but also on the relative difference between the aromaticity of the asphaltene and maltenes phase.⁶ The lower the difference, the higher is the feed stability. Thermal cracking increases the aromaticity of the asphaltene,¹⁶ and as the reaction proceeds, the difference between the aromaticity of the maltenes phase and the asphaltenes increases.⁶ Thus, the stability reduces as the conversion increases. At a particular conversion level, the inherent equilibrium between the maltene and the asphaltene phases eventually breaks up resulting in an unstable visbroken residue. To study the extent of maximum conversion that can be achieved without causing instability, the stability of the visbroken residue (500+) was measured by the merit number test. Only the high viscosity feed of Haldia asphalt was not analyzed for the stability. Figure 12 shows the stability of VR (500+) at different conversion levels for VB Feed, AMSR, and AM Asphalt feeds. From this figure it is clear that (i) the stability reduces as the conversion increases and (ii) the maximum achievable conversion was found to be a

function of the asphaltene content. AMSR (asphaltene-6.5 wt %), VB Feed (asphaltene-7.72 wt %), and AM Asphalt (asphaltene-9.8 wt %) gave maximum conversions of 33.59, 28.52, and 26.28%, respectively, without causing instability in the visbroken product.

6. Reaction Kinetics

For the present study, the relevant kinetic scheme has been proposed by Mosby et al.¹⁸ for residue hydrotreating. However, it requires comprehensive experimental data in terms of a hard to crack portion and an easy to crack portion of the residue, and often the parametric sensitivity becomes a major issue for such networks. Hence in the present case, the feed was considered as a single lump and based on the boiling point distribution of the distillates obtained at different conversion levels, a series-parallel kinetic model (Figure 13) consisting of industrially important pseudo-components with seven rate parameters has been proposed. The distillates were lumped based on the analytical procedure being followed in the refineries where the products are classified into salable boiling cuts assigned as G, Ga, LGO, VGO and VR. Among these, G, Ga, and LGO were assumed to be in the vapor phase and to be stable products since their cracking requires a very high activation energy, and with visbreaking being a mild liquid phase cracking, the lower carbon molecules appear more difficult to crack under the covered severity range. Also, the linear rise in the yields of the G and Ga for all the feedstocks further supports the assumption. The nonlinear trend in the yields of VGO proves its secondary cracking with an

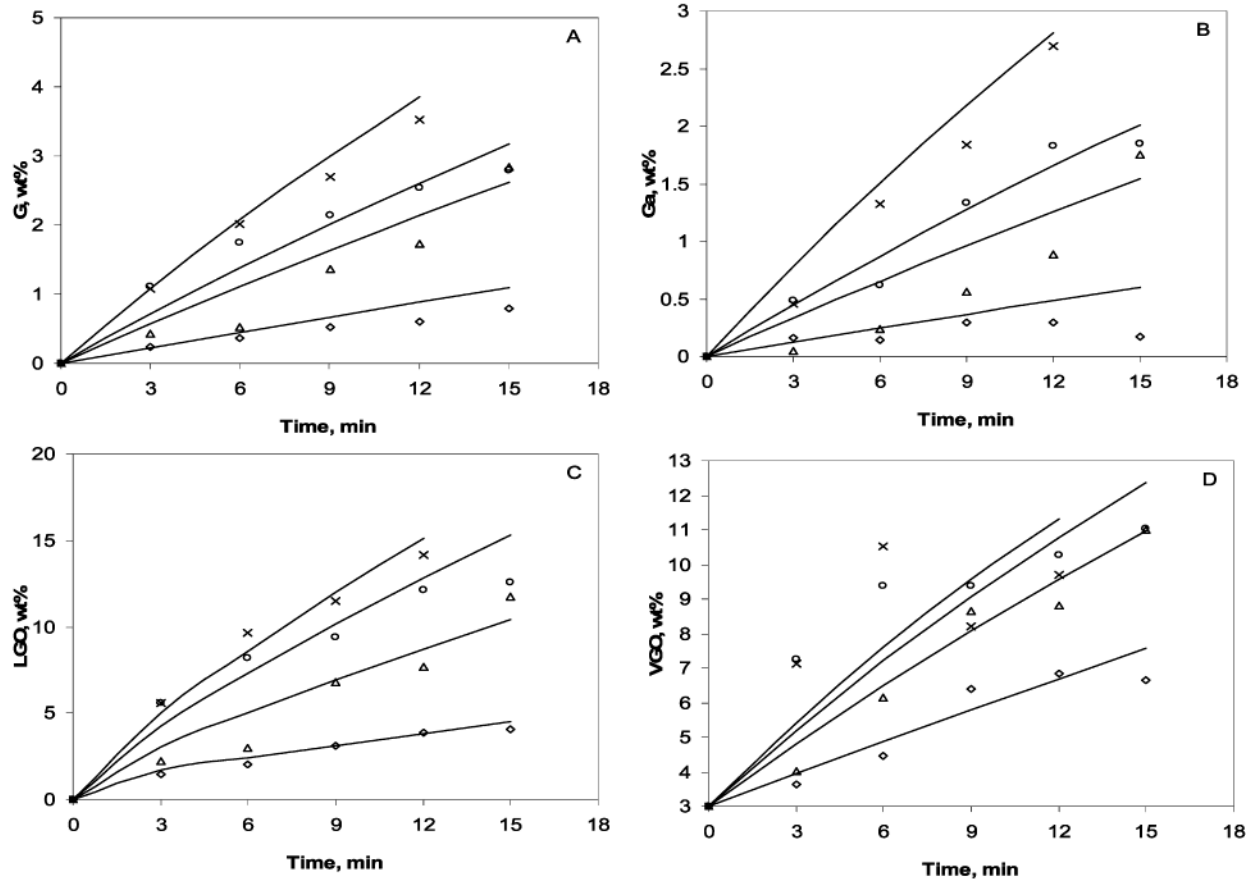


Figure 10. Comparison between experimental and predicted values of various components for AM Asphalt: (A) G; (B) Ga; (C) LGO; (D) VGO; \diamond , 400 °C; \triangle , 410 °C; \circ , 420 °C; \times , 430 °C.

increase in the severity and thus was taken into consideration during model development. It was observed that incorporating cracking of VGO to lighter products significantly improved the goodness of the fit. The exponential decline in the VR (500+) fraction with an increase in the severity shows that the cracking of residues follows first-order kinetics. Various reaction rates for different species can be given by the following set of first-order ordinary differential equations:

$$\frac{dVR}{dt} = -(k_1 + k_2 + k_3 + k_4)VR \quad (10)$$

$$\frac{dVGO}{dt} = k_4VR - (k_5 + k_6 + k_7)VGO \quad (11)$$

$$\frac{dLGO}{dt} = k_3VR + k_5VGO \quad (12)$$

$$\frac{dGa}{dt} = k_2VR + k_6VGO \quad (13)$$

$$\frac{dG}{dt} = k_1VR + k_7VGO \quad (14)$$

Equations 10–14 were integrated, and the obtained analytical solutions are

$$VR = VR_0 \exp(-k_{1234}t) \quad (15)$$

$$VGO = \frac{k_4VR_0}{(k_{567} - k_{1234})} [\exp(-k_{1234}t) - \exp(-k_{567}t)] + VGO_0 \exp(-k_{567}t) \quad (16)$$

$$LGO = \frac{k_3VR_0}{(k_{1234})} [1 - \exp(-k_{1234}t)] + \frac{k_5VGO_0}{(k_{567})} [1 - \exp(-k_{567}t)] + \frac{k_4k_5VR_0}{(k_{567} - k_{1234})} \left[\frac{1 - \exp(-k_{567}t)}{k_{567}} - \frac{1 - \exp(-k_{1234}t)}{k_{1234}} \right] + LGO_0 \quad (17)$$

$$Ga = \frac{k_2VR_0}{(k_{1234})} [1 - \exp(-k_{1234}t)] + \frac{k_6VGO_0}{(k_{567})} [1 - \exp(-k_{567}t)] + \frac{k_4k_6VR_0}{(k_{567} - k_{1234})} \left[\frac{1 - \exp(-k_{567}t)}{k_{567}} - \frac{1 - \exp(-k_{1234}t)}{k_{1234}} \right] + Ga_0 \quad (18)$$

$$G = \frac{k_1VR_0}{(k_{1234})} [1 - \exp(-k_{1234}t)] + \frac{k_7VGO_0}{(k_{567})} [1 - \exp(-k_{567}t)] + \frac{k_4k_7VR_0}{(k_{567} - k_{1234})} \left[\frac{1 - \exp(-k_{567}t)}{k_{567}} - \frac{1 - \exp(-k_{1234}t)}{k_{1234}} \right] + G_0 \quad (19)$$

where $k_{1234} = k_1 + k_2 + k_3 + k_4$ and $k_{567} = k_5 + k_6 + k_7$ are the lumped rate constants and VR_0 , VGO_0 , LGO_0 , Ga_0 , and G_0 are the initial concentrations of the different species at zero time.

6.1. Estimation of Reaction Rate Parameters. The values of rate constants were estimated by the

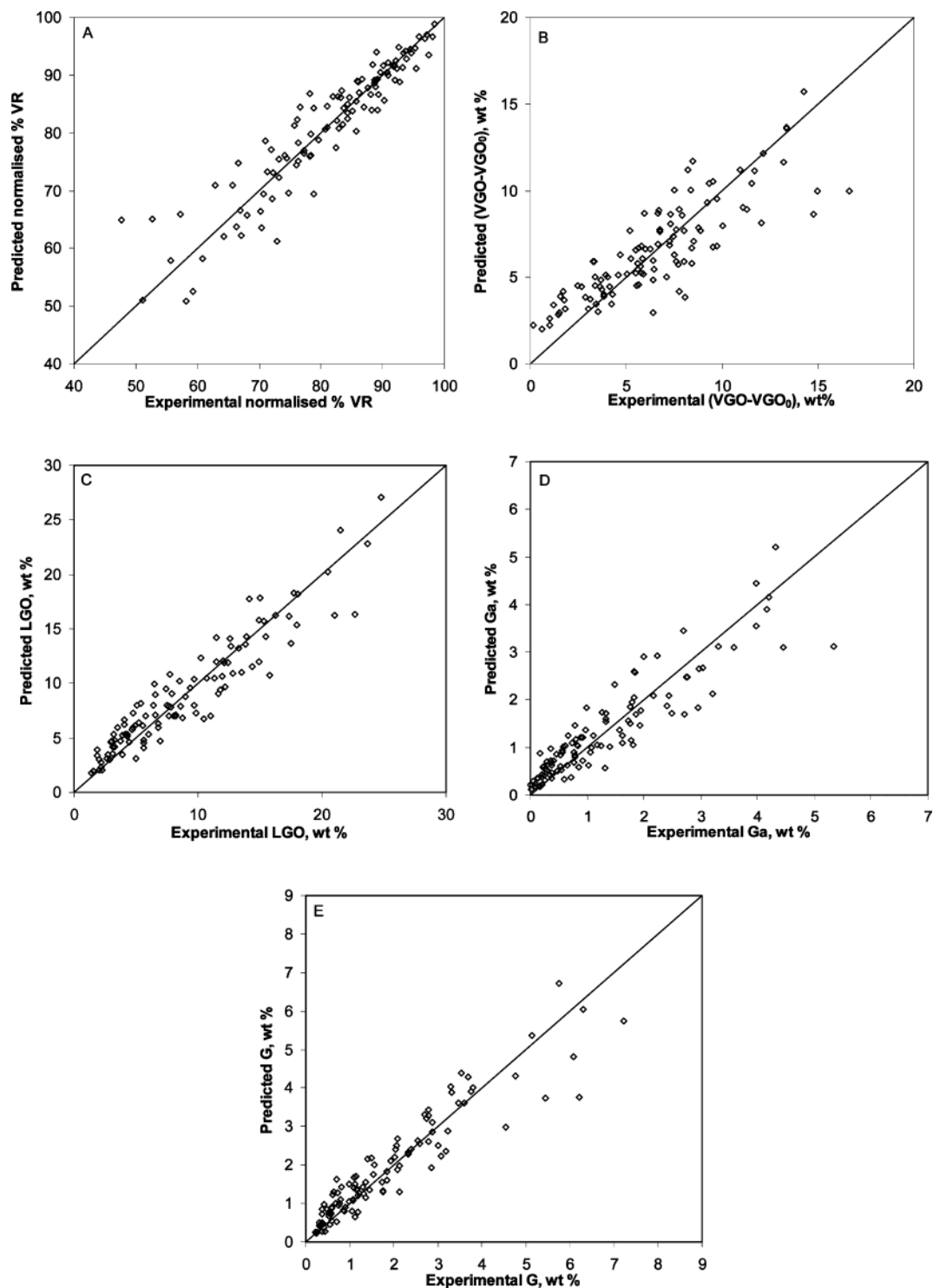


Figure 11. Parity plot for different components: (A) VR; (B) VGO; (C) LGO; (D) Ga; (E) G.

minimization of sum of square of errors (SSE) using constrained optimization algorithms. The objective function is given by

$$SSE = \sum_{i=1}^m \sum_{j=1}^n (y_{\text{exp}_{ij}} - y_{\text{pred}_{ij}})^2 \quad (20)$$

The good guess values for the rate constants were obtained by using Luus and Jaakola¹⁹ direct search derivative free optimization procedure. This procedure uses random search points and systematic contraction of the search region. Further, the converged solution

values were used as an initial guess for modified steepest descent method²⁰ to obtain optimized rate constants. The comparison of experimental and predicted values for each of the pseudo-component and for different feeds can be seen in Figures 4–10. Tables 5 and 6 give the estimated values of first-order reaction rate constants, activation energy and the frequency factor for each of the reaction path considered in the scheme. A careful analysis of the above tables points out the following observations:

1. At 400 °C, the higher k_4/k_{567} ratio suggests VGO, LGO, Ga, and G were essentially formed from VR while,

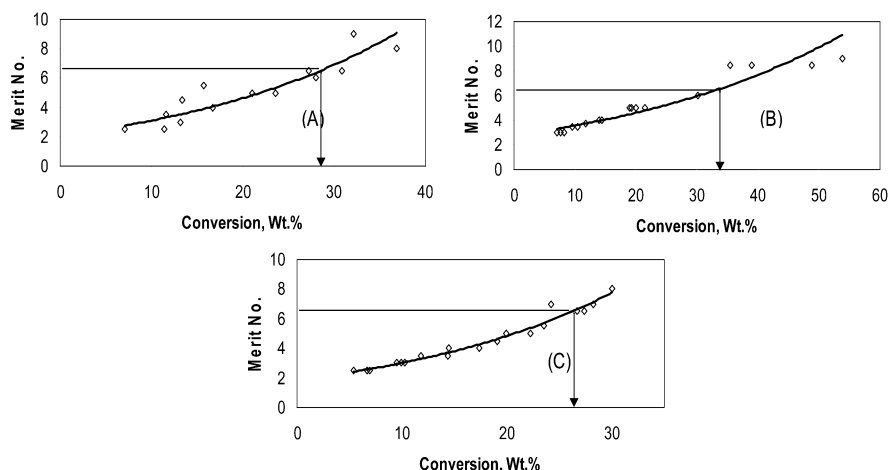


Figure 12. Stability of the feed at different conversion levels: (A) VB Feed; (B) AMSR; (C) AM Asphalt.

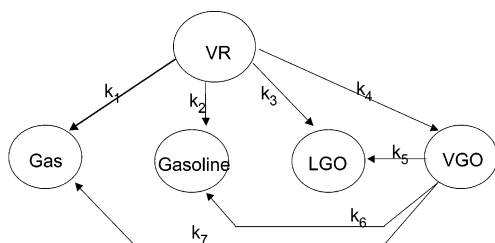


Figure 13. Proposed five lumped kinetic model with 10 rate parameters: VR, vacuum residue (500 °C+); G (C₁–C₅); Ga (IBP–150 °C); LGO (150–350 °C); VGO (350–500 °C).

Table 5. Global Kinetics (s⁻¹) for the Visbreaking of Residues and Asphalts

rate constants × 10 ⁵	NGSR	BHSR	AMSR	VB Feed	Haldia Asphalt	AM Asphalt
400 °C						
k ₁	1.96	0.744	1.25	1.74	nd ^a	1.32
k ₂	0.579	0.867	1.06	1.63	nd	0.714
k ₃	7.09	5.71	8.60	11.5	nd	4.20
k ₄	9.41	8.88	7.02	5.94	nd	5.52
k ₅	1.39	0.626 × 10 ⁻⁴	0.512	0.283	nd	0.275
k ₆	1.4	0.626 × 10 ⁻⁴	0.025	0.113	nd	0.0795
k ₇	0.029	0.626 × 10 ⁻⁴	0.142	0.202	nd	0.0602
410 °C						
k ₁	2.8	2.04	1.84	3.42	2.39	3.28
k ₂	1.15	1.87	1.23	3.54	2.16	1.90
k ₃	13.5	12.60	10.4	19.7	10.30	11.9
k ₄	13.2	9.80	9.11	9.79	13.60	10.90
k ₅	1.66	1.80	6.45	0.736	1.15	3.85
k ₆	1.41	0.167	1.10	0.167	1.78	1.22
k ₇	0.201	0.165	1.16	0.343	1.54	1.31
420 °C						
k ₁	4.62	4.53	7.01	4.98	4.61	4.14
k ₂	2.52	4.35	4.78	5.14	2.42	2.59
k ₃	22.6	25.40	28.30	24.60	19.90	19.30
k ₄	20.8	22.70	21.50	12.60	20.30	13.30
k ₅	2.23	3.89	7.92	1.03	1.38	2.08
k ₆	2.01	0.98	1.27	0.575	2.15	1.54
k ₇	2.51	0.12	1.37	2.63	2.23	1.75
430 °C						
k ₁	nd	9.45	12.50	8.12	11.00	6.37
k ₂	nd	6.7	9.82	7.06	10.90	4.60
k ₃	nd	39.70	54.60	34.50	31.10	23.70
k ₄	nd	20.30	47.90	17.50	32.20	14.80
k ₅	nd	7.51	10.90	2.86	3.62	2.47
k ₆	nd	2.42	0.973	2.84	5.86	1.97
k ₇	nd	4.33	6.69	3.57	7.50	2.06

^a nd = not determined.

at 410 °C, this ratio sharply decreased and from there on remained constant across some mean value except for VB Feed, which still showed a gradual fall. Thus,

Table 6. Arrhenius Parameters E (kcal mol⁻¹) and A (s⁻¹) for the Thermal Cracking Studies on Residues and Asphalts

param	k ₁	k ₂	k ₃	k ₄	k _{5/6/7}
NGSR					
E	39.74	68.21	53.65	36.77	40.27
A	1.54×10^8	8.05×10^{16}	1.92×10^{13}	8.01×10^6	3.08×10^8
BHSR					
E	79.24	65.68	61.33	31.24	90.66
A	4.31×10^{20}	1.95×10^{16}	5.08×10^{15}	1.2×10^6	2.25×10^{24}
AMSR					
E	77.59	75.47	61.38	62.06	95.69
A	1.71×10^{20}	2.68×10^{19}	6.14×10^{15}	8.41×10^{15}	1.49×10^{26}
VB Feed					
E	46.98	45	33.10	32.82	88.79
A	3.36×10^{10}	7.54×10^9	6.92×10^6	2.85×10^6	3.79×10^{23}
Haldia Asphalt					
E	72.76	76.92	52.73	41.23	63.44
A	4.43×10^{18}	7.06×10^{19}	7.95×10^{12}	2.09×10^9	7.79×10^{15}
AM Asphalt					
E	46.70	55.55	53.62	29.76	76.67
A	1.36×10^{12}	5.39×10^{14}	1.14×10^{13}	2.97×10^5	7.15×10^{19}

cracking reactions of VGO species are more significant at higher temperatures.

2. The reaction rate constants for AMSR are higher as compared to those for AM Asphalt (obtained by deasphalting of AMSR). This may be explained as the fact that deasphalting of vacuum residue causes the removal of the maltene phase (easy to crack portion of the residue) and a consequent increase in the asphaltene content (AMSR 6.5%, AM Asphalt 9.61%) of the feed. Such a refractory feed is hard to crack and thus shows lower conversions.

3. In the case of BHSR, AMSR, VB Feed, and Haldia Asphalt, the activation energies E_4 and E_3 (VR to VGO and LGO formation) are lower as compared to the E_1 and E_2 energies (VR to G and Ga formation). This suggests a C–C splitting reaction of saturates and naphthenic aromatics (present as major components) to dominate over the dealkylation reactions that occur in the asphaltenes and polar aromatics (minor components). This is in accordance with the cracking path followed by the components showed earlier. However for NGSR and AM Asphalt, the estimated values of E_1 and E_4 were lower than E_2 and E_3 . This suggests that, for these feeds, the tendency toward G and VGO formation is higher as compared to the Ga and LGO formation.

4. The activation energy for VGO cracking was found to be in the range of 63–95 kcal/mol except for NGSR,

which showed exceptionally lower activation energy (40.27 kcal/mol). This suggests lower secondary cracking of VGO to light ends under the covered severity range.

5. The comparison of compositionally related feeds such as VB Feed and AMSR showed a large variation in the activation energy and for the same reaction paths (VR to VGO, LGO, Ga, and G) the frequency factors varied as much as 10^{11} orders of magnitude.

The last point draws our attention to some of the pitfalls of the lumping and kinetic scheme described by Weekaman²¹ and Quann and Jaffe,²² which can be restated as follows: (i) While lumping of many series and parallel first-order reactions, the recycle streams must be lumped with different rate expressions as they may change the overall rate constants and consequently the activation energies. (ii) The lumping approach often fails to extrapolate to the different feedstocks because of the compositional differences within the same defined lumps. (iii) The actual composition of the lumps may change in terms of molecular components with overall conversion of the system and mask the true kinetics. (iv) The approach based on the boiling point range lacks a convenient method to incorporate the reaction chemistry at the molecular level and multiple property information. Until the cracking behavior of feed at molecular level is understood, with the above pitfall of lumped reaction models, the feed dependency over the rate parameters can be semiquantitatively obtained.

6.2 Variation in Activation Energies with Feed Properties. An attempt has been made to correlate the estimated activation energies with the feed properties. It was observed that no single property individually could predict the variation in the activation energies; instead, a cumulative property (in the dimensionless form) depicted the dependency. Among the different correlations tested the linear and power-law type models gave satisfactory results for VR to products (Figure 14).

1. The activation energy for cracking of VR to VGO (E_4) was found to be a function of the nC_5 , CCR, and S content of the feed except for the case of AMSR as

$$E_4 = 27.67 \left(\frac{nC_5}{S + CCR} \right) + 16.636 \quad (R^2 = 0.98) \quad (21)$$

The above relationship shows that the feeds rich in the maltene phase (nC_5 soluble) due to the prevalence of splitting reactions leads to higher selectivity toward VGO formation. The CCR term included in the expression indicates feed aromaticity and heteroatom content (especially sulfur moieties), which are supposed to be free radical initiators, reduce the activation energy with their presence.^{23,24}

The activation energy for VR to G was found to depend on As, NP, and PA (except for VB Feed) as

$$E_1 = 33.59 \left(\frac{As + NA}{PA} \right)^{0.33} \quad (R^2 = 0.91) \quad (22)$$

It indicates that the formation of G depends on the ratio of the components having side chains on their polycondensed cores in different proportion by dealkylation reactions.

3. The activation energy for VR to Ga formation was found to depend on the ratio of resins (Rs, obtained by the difference of nC_5 and nC_7 insoluble) and asphaltene (As, nC_7 insoluble) content of the feed with the following relationship:

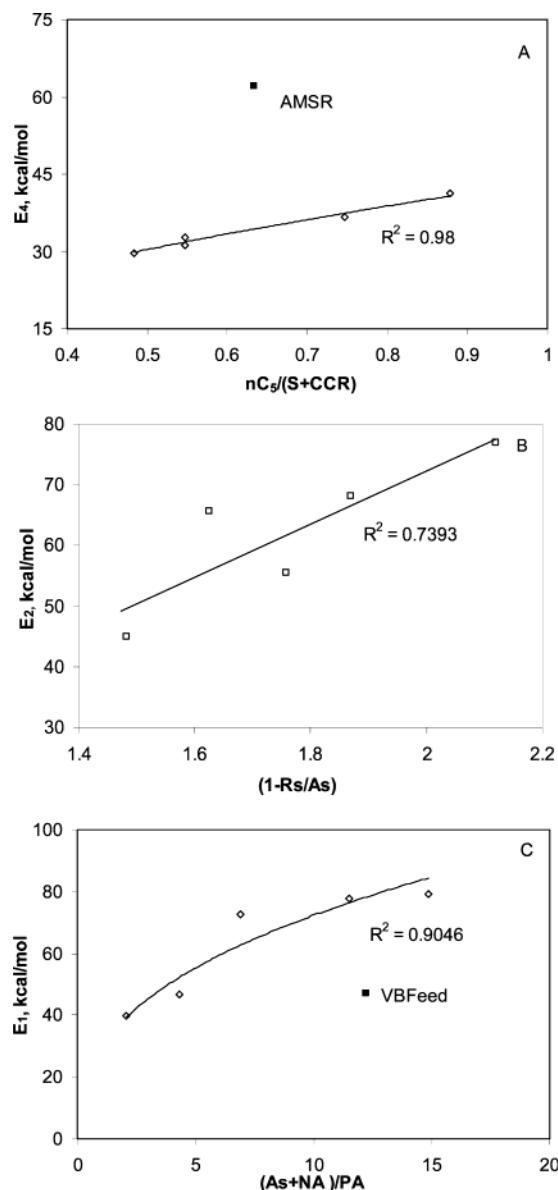


Figure 14. Correlations between activation energy and feed properties: (A) VR to VGO, E_4 ; (B) VR to Ga, E_2 ; (C) VR to G, E_1 .

$$E_2 = 43.51 \left(1 + \frac{Rs}{As} \right) - 14.79 \quad (R^2 = 0.74) \quad (23)$$

4. In the case of LGO, due to lack of an appreciable difference in the estimated activation energy (± 5 kcal/mol, except the VB Feed, which showed substantially lower activation energy) among studied feeds, no specific dependency could be obtained.

It can be concluded that the difference in the characteristics of the residue composition induces the variation in the kinetic results. For further improvement in the above correlations, simultaneous variation in the structural properties of different component class and their reactivity changes in the feed that are likely to occur during its thermal processing should also be studied.

7. Conclusions

(1) Within the studied range, all the feeds were found to undergo thermal cracking to give gas and distillates, and no coke formation was observed.

(2) For a given feed, the composition of the gas fraction was found to remain practically unchanged at any severity with methane present as a major constituent.

(3) The stability of the feed decreases with increasing conversion of VR. The maximum permissible conversion (crackability of the feed) was found to be the function of the asphaltene content.

(4) G, Ga, and LGO were found to be stable products; however, VGO significantly undergoes cracking at higher severity.

(5) The crackability of the vacuum residue was found to be higher than its corresponding asphalt.

(6) The five-lumped series-parallel kinetic scheme with seven kinetic parameters developed could adequately capture the essential mechanism of the thermal cracking reactions occurring during the visbreaking operation.

(7) The product yields and their activation energies were found to be the function of the severity and feed characteristics.

Acknowledgment

The authors are thankful to the Centre for High Technology, Government of India, for providing the financial help and also to Indian Institute of Petroleum, Dehradun, India, for providing the experimental and analytical facilities.

Nomenclature

A = frequency factor, s^{-1}

As = asphaltenes (n -heptane insolubles), wt %

E = activation energy, kcal/mol

G = gas (C_1 – C_5), wt %

G_a = gasoline (boiling range IBP–150 °C), wt %

G_{a0} = initial concentration of gasoline component at zero residence time, wt %

G_o = initial concentration of gas component at zero residence time, wt %

k_i = first-order rate constant for i th species, s^{-1}

LGO = light gas oil (boiling range 150–350 °C), wt %

LGO_o = initial concentration of light gas oil component at zero residence time, wt %

NA = naphthenic aromatics, wt %

nC_5 = n -pentane insolubles, wt %

nC_7 = n -heptane insolubles, wt %

PA = polar aromatics, wt %

R = gas constant, 1.987 kcal/(mol K)

Rs = resins, wt %

Sa = saturates, wt %

t = time, s

T_{700} = reference temperature used in eq 4, K

VGO = vacuum gas oil (boiling range 350–500 °C), wt %

VGO_o = initial concentration of vacuum gas oil component at zero residence time, wt %

VR = vacuum residue (500+)

VR_o = initial concentration of vacuum residue at zero residence time, wt %

W_{500-} = mass fraction of distillates (500–) components, g

W_{feed} = weight of feed, g

W_{gas} = weight of gas, g

W_i = weight of different species, g

y_i = variable

Subscripts

i = species G, Ga, LGO, VGO

Greek Letters

ρ_{av} = average gas density, kg/m³

Literature Cited

- (1) Shen, H.; Ding, Z.; Li, Rui. Thermal conversion—An efficient way for heavy residue processing. *Proc. 15th World Pet. Congr.* **1998**, 2, 907.
- (2) Akbar, M.; Geelen, H. Visbreaking uses soaker drum. *Hydrocarbon Process.* **1981**, May, 81.
- (3) Al Soufi, H. H.; Savaya, Z. F.; Moahammed, H. K.; Al-Azami, I. A. Thermal conversion (visbreaking) of heavy Iraqi residue. *Fuel* **1988**, 67, 1714.
- (4) Krishna, R.; Kuchhal, Y. K.; Sarna, G. S.; Singh, I. D. Visbreaking studies on Aghajari long residue. *Fuel* **1988**, 67, 379.
- (5) Castellanos, J.; Cano, L. J.; del Rosal, R.; Briones, V. M.; Mancilla, R. L. Kinetic model predicts visbreaker yields. *Oil Gas J.* **1991**, March 18, 76.
- (6) Di Carlo, S.; Janis, B. Composition and visbreakability of petroleum residues. *Chem. Eng. Sci.* **1992**, 47, 2675.
- (7) Benito, A. M.; Martinez, M. T.; Fernandez, I.; Miranda, J. L. Visbreaking of an asphaltic coal residue. *Fuel* **1995**, 74, 922.
- (8) Xiao, J.; Wang, L.; Chen, Q.; Wang, D. Modeling for product distribution in thermal conversion of heavy oil. *Pet. Sci. Technol.* **2002**, 20, 605.
- (9) Takatsuka, T.; Kajiyama, R.; Hashimoto, H. A practical model of thermal cracking of residual oil. *J. Chem. Eng. Jpn.* **1989**, 22, 304.
- (10) Del Bianco, A.; Anelli, P. M.; Beltrame, P. L.; Carniti, P. Thermal cracking of petroleum residues 1. Kinetic analysis of the reaction. *Fuel* **1993**, 72, 75.
- (11) Trauth, D. M.; Yasar, M.; Neurock, M.; Nigam, A.; Klien, M.; Kukes, S. G. Asphaltene and resid pyrolysis: Effect of reaction environment. *Fuel Sci. Technol. Int.* **1992**, 10, 1161.
- (12) Yasar, M.; Trauth, D. M.; Klien, M. Asphaltene and resid pyrolysis: Effect of reaction environment on pathways and selectivities. *Energy Fuels* **2001**, 15, 504.
- (13) Zhou, X.; Chen, S.; Ma, B.; Li, C.; Chang, K. Kinetic model for thermal conversion of vacuum residue. *Shiyou Xuabao, Shiyou Jiangong* **1999**, 15 (2), 79.
- (14) Singh, J. Ph.D. Thesis, Chem. Eng. Department, I.I.T., Roorkee, India, 2003.
- (15) Maxa, D.; Prochaska, F.; Sebor, G.; Blazek, J.; Kroufek, J. Comparison of vacuum residue visbreaking and hydrovisbreaking. *Pet. Coal* **2002**, 44 (1–2), 36.
- (16) Fainberg, V.; Podorozhansky, M.; Hetsroni, G.; Brauch, R.; Kalchouk, H. Changes in the composition and properties of the vacuum residues as a results of visbreaking. *Fuel Sci. Technol. Int.* **1996**, 14, 839.
- (17) Yan, Y. T. Characterization of visbreaker feed. *Fuel* **1990**, 69, 1062–1064.
- (18) Mosby, J. F.; Buttke, R. D.; Cox, J. A.; Nikolaides, C. Process characterization of expanded-bed reactors in series. *Chem. Eng. Sci.* **1986**, 41, 989–995.
- (19) Englezos, P.; Kalogerakis, N. *Applied parameter estimation for chemical engineers*, 1st ed.; Marcel Dekker: New York, 2001.
- (20) Biegler, L. T.; Damiano, J. J.; Blau, G. E. Nonlinear parameter estimation: a case study. *AIChE J.* **1986**, 32 (1), 29.
- (21) Weekman, V. W. Lump, models and kinetics in practice. *Chem. Eng. Prog. Monogr. Ser.* **1979**, 75 (11), 3–75.
- (22) Quann, R. J.; Jaffe, S. B. Structure-oriented lumping: Describing the chemistry of complex hydrocarbon mixtures. *Ind. Eng. Chem. Res.* **1992**, 31, 2483–2497.
- (23) Thomas, M.; Fixari, B.; Le Perche, P.; Princic, Y.; Lena, L. Visbreaking of safaniya vacuum residue in the presence of additives. *Fuel* **1989**, 68, 318–322.
- (24) Dente, M.; Bozzano, G.; Bussani, G. A comprehensive program for visbreaking simulation: product amounts and their properties prediction. *Comput. Chem. Eng.* **1997**, 21, 1125–1134.

Received for review July 7, 2003

Revised manuscript received December 30, 2003

Accepted December 30, 2003

IE0305723